

## Supplementary Information

### **Mesomorphic and photochromic luminescent behaviour of side-chain liquid crystalline polymers containing di-substituted cyanostilbene groups with the different number of alkyl tail chain**

Juan Luo, Juan Wang, Junde Zhang, Huiyi Cao and Xiaofang Chen\*

<sup>a</sup>Suzhou Key Laboratory of Macromolecular Design and Precision Synthesis, Jiangsu Key Laboratory of Advanced Functional Polymer Design and Application, State and Local Joint Engineering Laboratory for Novel Functional Polymeric Materials, College of Chemistry, Chemical Engineering and Materials Science, Soochow University, Suzhou 215123, P. R. China.

E-mail: [xfchen75@suda.edu.cn](mailto:xfchen75@suda.edu.cn) .

## Experimental section

### Materials

4-Hydroxy benzaldehyde (AR 98%), Protocatechualdehyde (98%), 3,4,5-Trihydroxybenzaldehyde (98%), 1-Bromododecane (97%), Potassium iodide (99%), Methyl 4-(cyanomethyl)benzoate (98.87%), Methyl 2,3-dihydroxybenzoate (99.83%), 1-[3-(Dimethylamino) propyl]-propyl]-3-ethylcarbodiimide hydrochloride (EDC·HCl, 99%), 4-(Dimethylamino) pyridine (DMAP, 99%), and Grubbs catalyst (third generation) were purchased from Sigma Aldrich. Dichloromethane (CH<sub>2</sub>Cl<sub>2</sub>) (AR, Sinopharm) and Trichloromethane (CHCl<sub>3</sub>) (AR, Sinopharm) were distilled by refluxing over CaH<sub>2</sub> prior to use. Tetrahydrofuran (THF) (AR, Sinopharm) was heated under reflux over sodium for at least 8 h and distilled before use. N-(6-hydroxyhexyl)-cis-5-nor-bornene-exo-2,3-dicarboximide were prepared according to literature procedure. All other reagents and solvents were obtained from commercial sources and used without further purification.

### Measurements

**Nuclear Magnetic Resonance Spectroscopy (NMR)** The <sup>1</sup>H and <sup>13</sup>C NMR spectra were recorded on an Agilent 600 MHz NMR spectrometer at ambient temperature with CDCl<sub>3</sub> as solvent and tetramethylsilane (TMS) as internal standard.

**Mass Spectrometry (MS)** MS spectra of photoproducts were recorded on matrix-assisted laser desorption/ionization time-of-flight (MALDI-TOF) mass spectrometer (Ultra extreme, Bruker Co.).

**Gel Permeation Chromatography (GPC)** The number-average molecular weight (M<sub>n</sub>) and polydispersity (PDI) of polymers were measured on an instrument comprised of a Waters 1515 isocratic HPLC pump, a Waters 717 plus auto sampler, a Waters 2414 refractive-index detector with three 300 mm (length) × 7.5 mm (inner diameter) columns with a particle size of 5 μm (PL gel mixed-C, Polymer Laboratories). THF was used as the eluent at a flow rate of 1.00 mL/min at 35 °C. The calibration was carried out with a series of polystyrene standards.

**Infrared spectrometer (IR)** IR spectra were measured on an attenuated total reflection Fourier transform infrared spectroscopy (ATR-FTIR) (Bruker Vertex 70).

**Thermogravimetric Analysis (TGA)** The thermal stability of all polymers was measured by TGA on a TGA55 instrument at a heating rate of 10 °C /min from room temperature to 800 °C under a nitrogen atmosphere.

**Differential Scanning Calorimetry (DSC)** Thermal behavior and phase transition temperatures of all monomers and polymers were observed and obtained using a DCS 250 instrument. The temperature and heat flow were calibrated using standard materials (indium and zinc) at a cooling and heating rate of 10 °C /min. Samples with a typical mass of about 6 mg were encapsulated in sealed aluminum pans. The DSC curves recorded their first cooling and second heating processes at a rate of 10 °C /min.

**Polarized Optical Microscopy (POM)** LC textures and birefringence of samples were examined under an Olympus BX51-P microscope equipped with a Linkam THMS 600 hot stage. Samples were made by sandwiching the polymer powder between a glass slide and a cover glass. These samples were heated to their isotropic temperature and cooled at a rate of 1 °C/min.

**Small Angle X-ray Scattering (SAXS)** To identify phase structures of polymers, SAXS

experiments were performed using a high-flux X-ray instrument (SAXSess mc<sup>2</sup>, Anton Paar) equipped with Kratky block-collimation system and a GEID3003 sealed-tube X-ray generator (CuK $\alpha$ ). The wavelength is 0.1542 nm. Samples were wrapped into aluminum foils and sandwiched in a steel sample holder. The X-ray scattering patterns were recorded in vacuum on an imaging-plate (IP) which extended to high-angle range (the  $q$  range covered from 0.06 to 29 nm<sup>-1</sup>,  $q = 4\pi(\sin\theta)/\lambda$ , where the  $\lambda$  is the wavelength of 0.1542 nm and  $q$  is the scattering vector). The diffraction peak positions were calibrated with silver behenate.

**Photoluminescence Spectroscopy** PL spectra of solutions and solids were recorded on a RF-6000, with excitation wavelength of 350 nm for solids, 335 nm for solutions.

**UV-Vis Spectroscopy** UV-Vis spectra of solids were recorded on a Shimadzu UV3600 spectrophotometer.

**Absolute PL Quantum Yield Spectrometer (PLQY)** The fluorescence absolute values of  $\Phi_F$  were obtained on a Hamamatsu QY-Plus C13534-11 with an integrating sphere.

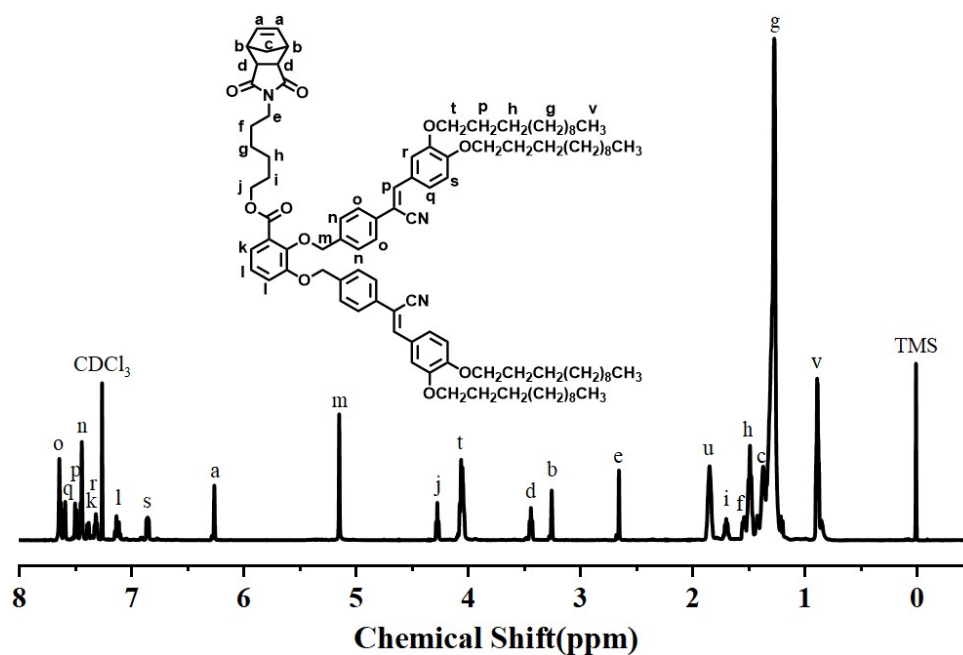


Fig. S1 <sup>1</sup>H NMR spectrum of NB-Z-34 in CDCl<sub>3</sub>.

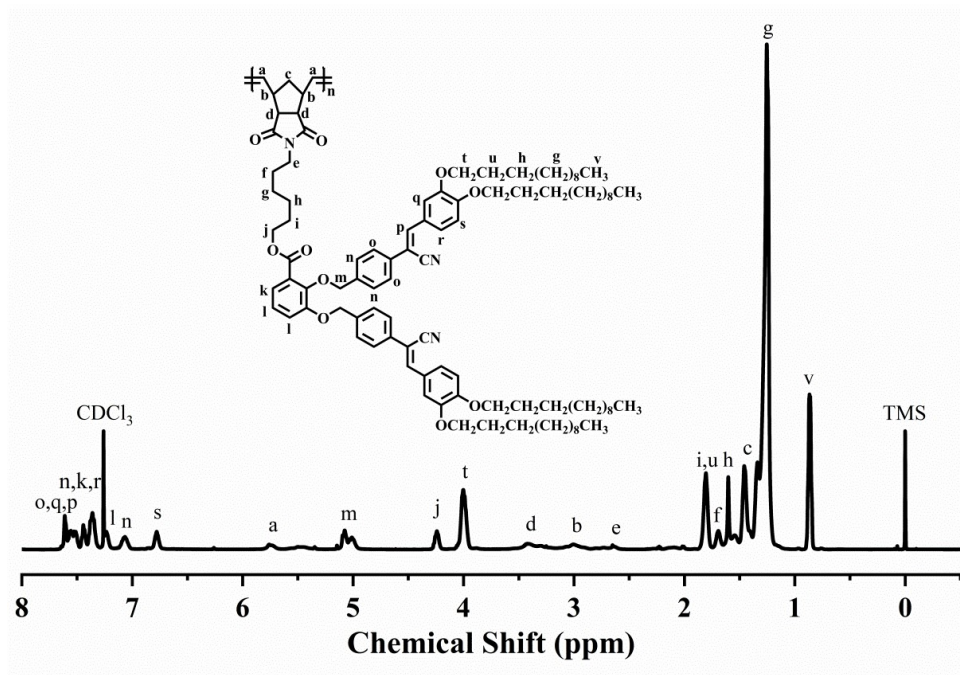


Fig. S2 <sup>1</sup>H NMR spectrum of PNB-Z-34 in CDCl<sub>3</sub>.

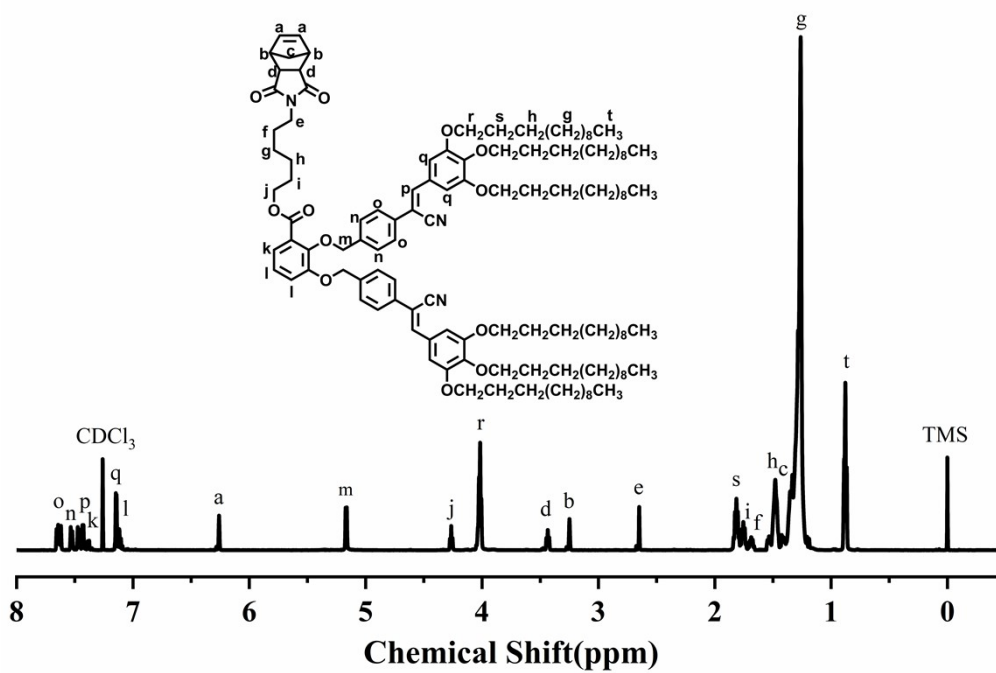


Fig. S3 <sup>1</sup>H NMR spectrum of NB-Z-345 in CDCl<sub>3</sub>.

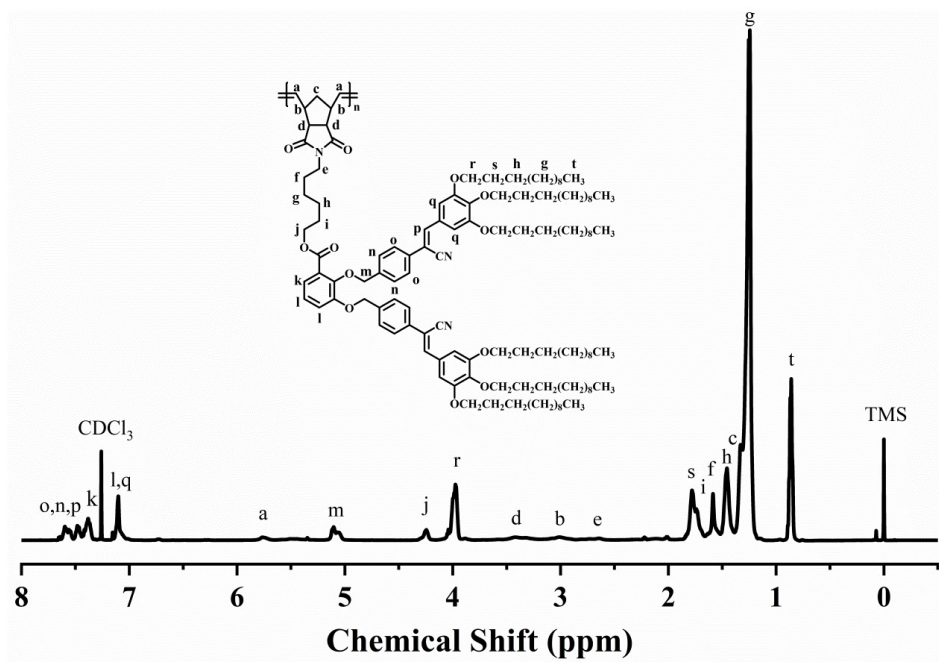


Fig. S4  $^1\text{H}$  NMR spectrum of PNB-Z-345 in  $\text{CDCl}_3$ .

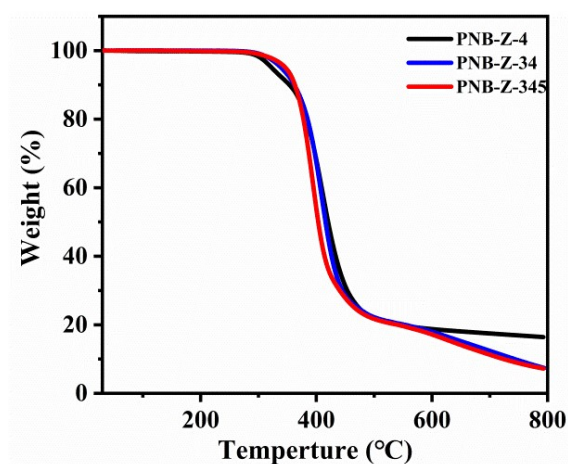


Fig. S5 TGA curves of PNB-Z-4, PNB-Z-34 and PNB-Z-345.

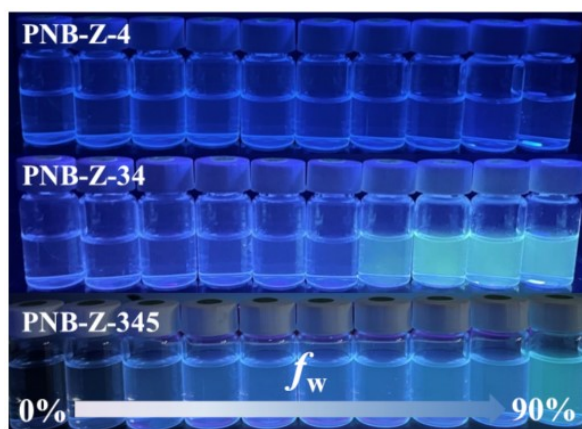
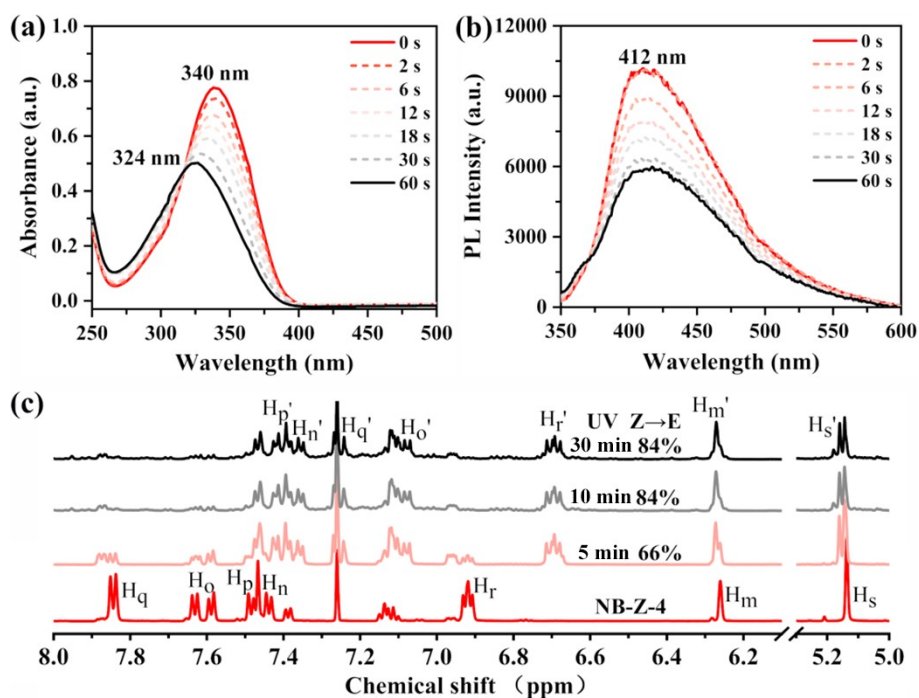
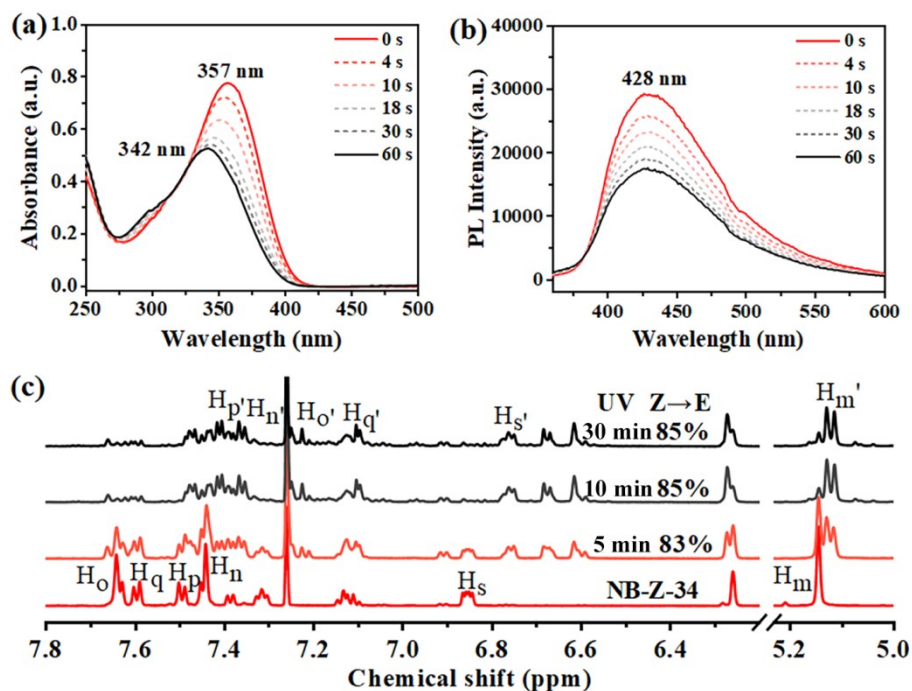


Fig. S6 Fluorescence pictures of PNB-Z-4, PNB-Z-34 and PNB-Z-345 in  $\text{THF}/\text{H}_2\text{O}$  with  $f_w$  from 0% to 90% under 365 nm UV light.



**Fig. S7** UV-Vis spectra (a) and PL spectra (b) of NB-Z-4 in  $\text{CHCl}_3$  before and after 365 nm UV irradiation for different time ( $c = 2 \times 10^{-5} \text{ mol} \cdot \text{L}^{-1}$ ). (c)  $^1\text{H}$  NMR spectra of NB-Z-4 in  $\text{CDCl}_3$  before and after UV irradiation for 5 min, 10 min and 30 min.



**Fig. S8** UV-Vis spectra (a) and PL spectra (b) of NB-Z-34 in  $\text{CHCl}_3$  before and after 365 nm UV irradiation for different time ( $c = 2 \times 10^{-5} \text{ mol} \cdot \text{L}^{-1}$ ). (c)  $^1\text{H}$  NMR spectra of NB-Z-34 in  $\text{CDCl}_3$  before and after UV irradiation for 5 min, 10 min and 30 min.



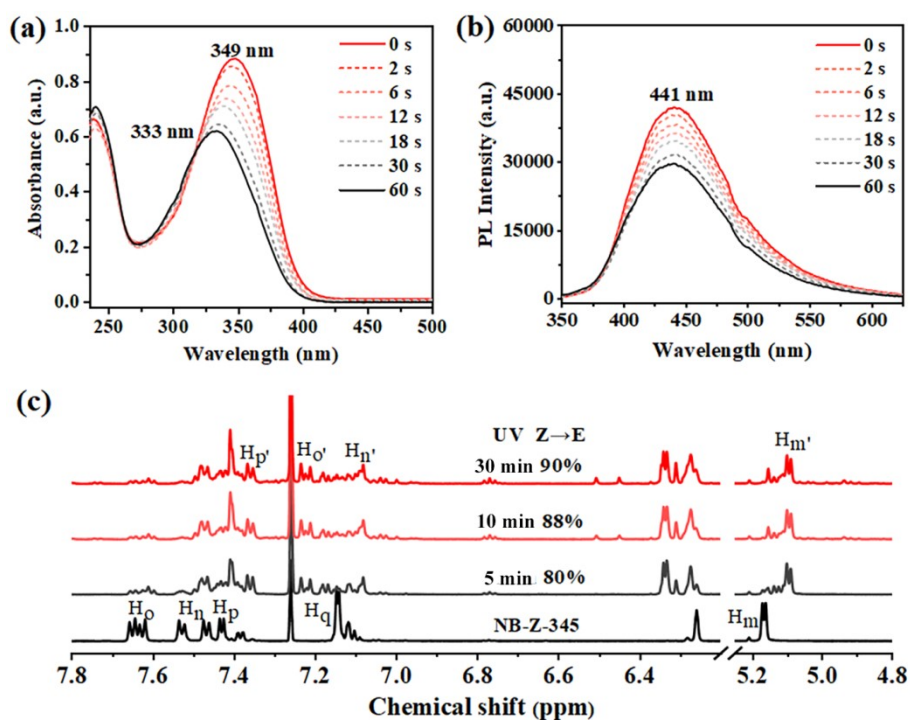


**Fig. S9** UV-Vis spectra (a) and PL spectra (b) of NB-Z-345 in  $\text{CHCl}_3$  before and after 365 nm UV irradiation for different time ( $c = 2 \times 10^{-5} \text{ mol} \cdot \text{L}^{-1}$ ). (c)  $^1\text{H}$  NMR spectra of NB-Z-345 in  $\text{CDCl}_3$  before and after UV irradiation for 5 min, 10 min and 30 min.

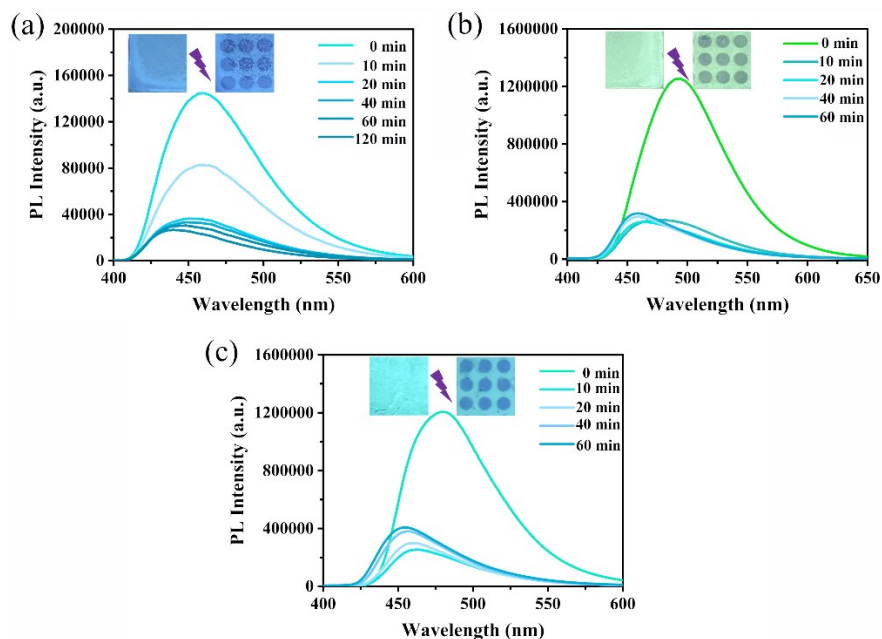


**Fig. S10** PL spectra change of NB-Z-4 (a), NB-Z-34 (b) and NB-Z-345 (c) films under 365 nm UV irradiation for different time. (inset: Fluorescent pictures of the initial monomer films (left) and irradiated monomer films with photomask for 60 min (right)).

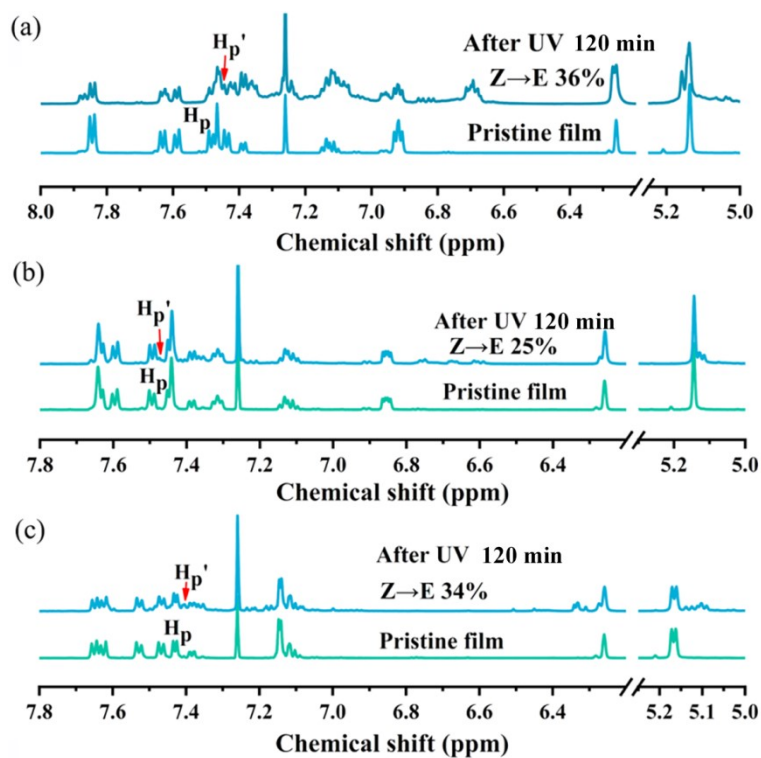


**Fig. S11**  $^1\text{H}$  NMR spectra of NB-Z-4 (a), NB-Z-34 (b) and NB-Z-345 (c) films before and after UV irradiation for 120 min.

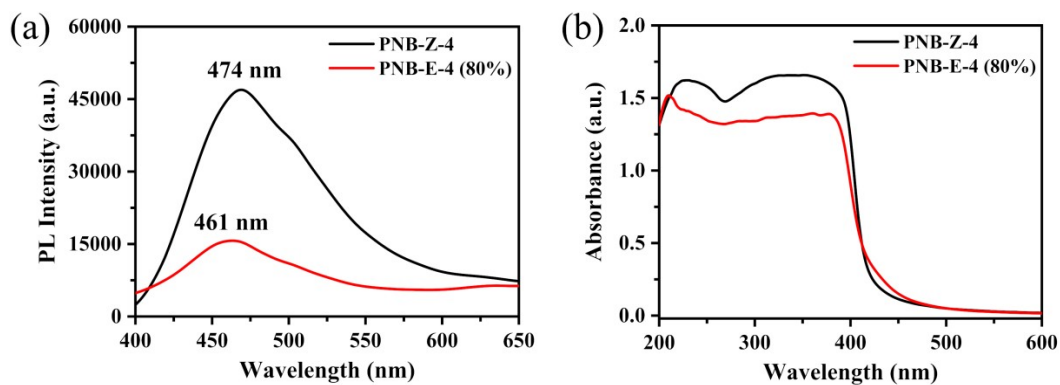


**Fig. S12** UV-Vis spectra (a) and PL spectra (b) of pristine and “irradiated” PNB-Z-4 film (The content of PNB-E-4 is more than 80%).



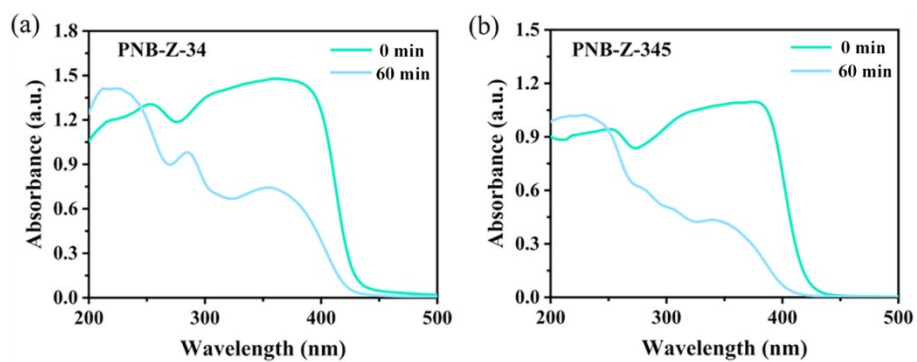


**Fig. S13** UV-Vis spectra of PNB-Z-34 (a) and PNB-Z-345 (b) films before and after UV irradiation.

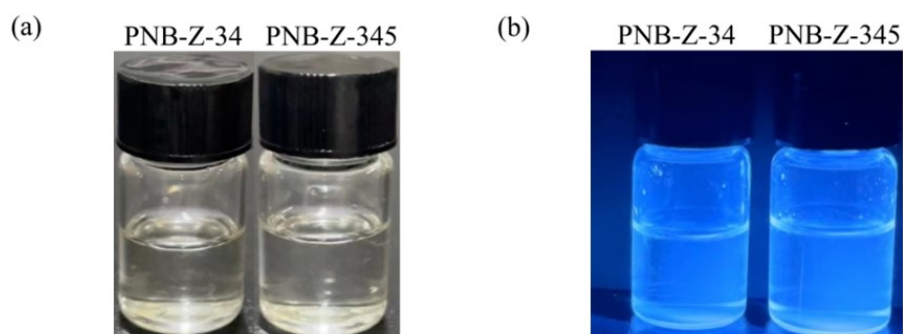


**Fig. S14** Dissolution of irradiated PNB-Z-34 and PNB-Z-345 films in  $\text{CHCl}_3$  under daylight (a) and UV light (b).

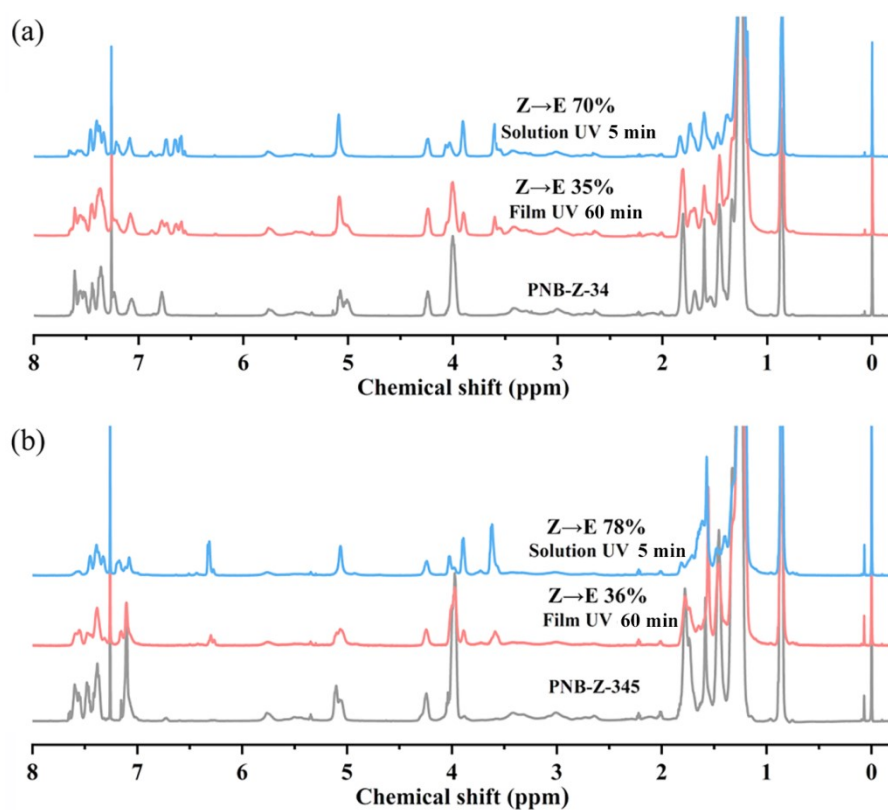


**Fig. S15**  $^1\text{H}$  NMR spectra of PNB-Z-34 (a) and PNB-Z-345 (b) solution and films before and after UV irradiation.

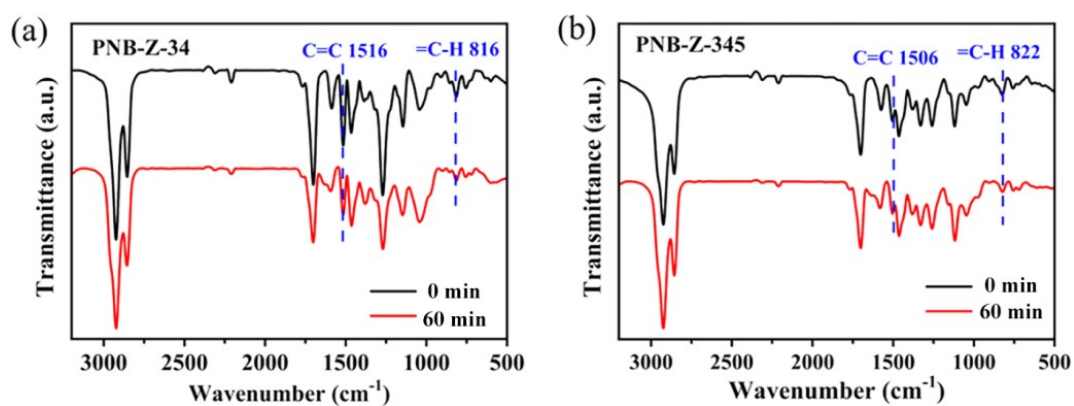


**Fig. S16** FT-IR spectra of PNB-Z-34 (a) and PNB-Z-345 (b) film before and after irradiation.